

Research Article

Analysis of the Influence of Slope Sliding on the Stability of Underground Diaphragm Wall Bridge Foundation Based on Wireless Sensor Network

Lijuan Wang  and Qihua Zhao

State Key Laboratory of Geohazard Prevention and Geoenvironment Protection (Chengdu University of Technology),
Sichuan Chengdu 610059, China

Correspondence should be addressed to Lijuan Wang; 2016010055@stu.cdut.edu.cn

Received 4 July 2022; Revised 22 July 2022; Accepted 30 July 2022; Published 13 August 2022

Academic Editor: Gengxin Sun

Copyright © 2022 Lijuan Wang and Qihua Zhao. This is an open access article distributed under the Creative Commons Attribution License, which permits unrestricted use, distribution, and reproduction in any medium, provided the original work is properly cited.

Real-time monitoring, condition assessment, early warning processing, and damage identification of underground diaphragm wall bridge structures are the current research trends. Based on the wireless sensor network theory, this paper constructs the stability model of the slope sliding on the underground diaphragm wall bridge foundation. The model builds a complete set of underground diaphragm wall bridge vibration signal acquisition and monitoring platform through wireless sensor network node data acquisition and solves the problem of data accuracy measurement by using theoretical analysis, software and hardware design, software simulation, and experimental verification methods. During the simulation process, experiments were designed such as slope sliding vibration signal acquisition data accuracy test, sensor node wireless charging power test and modeling, lithium battery charging power test and modeling, wireless rechargeable sensor node system work test, and other experiments. The experimental results show that the accuracy of the collected vibration signals of the underground diaphragm wall bridge is high, the main working frequency bands are 868 MHz, 915 MHz, and 2.4 GHz, the maximum data transmission rate is 250 Kbps, and the communication distance reaches 100 m, which can meet the requirements of the underground diaphragm wall. The power of wireless charging of lithium batteries reaches 4.5 mW, which effectively improves the stability measurement accuracy of underground diaphragm wall bridge foundations.

1. Introduction

As an important transportation hub, the safe operation of underground diaphragm wall bridges is related to the safety of people's lives and property and the country's economic construction. Real-time monitoring and evaluation of the health status of underground diaphragm wall bridges have important practical significance and application value [1]. In recent years, the application of wireless sensor network in the structural health monitoring of underground diaphragm wall bridges has become a research hotspot in this field. Its convenient installation, low maintenance cost, and flexible deployment make the monitoring system based on wireless sensor network gradually replace the traditional monitoring system [2], but wireless sensor network nodes

still have certain limitations in data processing and energy supply [3].

Under the background of the increasingly complex and technically difficult design of the underground diaphragm wall bridge structure, the safety of the underground diaphragm wall bridge structure has become a very worthy of research and attention [4–6]. It is closely related to the economic construction of the country and the life of social individuals. Since the beginning of the new century, major safety accidents such as the collapse of large-scale underground diaphragm wall bridges and the rupture of bridge decks have occurred frequently all over the world, posing a great threat to the safety of people's lives and property [7]. Therefore, if the status of the underground diaphragm wall bridge structure can be monitored in a timely manner and

the damage can be identified, processed, and even repaired in time, the safety of the underground diaphragm wall bridge structure can be greatly improved, and many disasters can be avoided and has very important practical significance and application value [8].

Aiming at the acquisition, storage, and wireless transmission of non-high-frequency vibration signals of bridge structure systems in the field of underground diaphragm wall bridge health monitoring, this paper first designs wireless sensor network nodes from the hardware framework and software program. Adhering to the principle of “low power consumption, low cost and high precision,” the designed wireless sensor network nodes include microcontroller modules, ICP (Inductively Coupled Plasma) acceleration sensor modules, wireless communication modules, and energy supply modules. In order to facilitate the operator to use the wireless sensor network node to collect the vibration signal of the underground diaphragm wall bridge and also for better experimental verification, this paper also designs a set of host computer software based on this wireless sensor network node. After the coordinator receives it, it is sent to the computer through the serial port. The vibration data of the bridge deck is collected by the acceleration sensor, and then, the sampled data is transmitted in the form of data packets. Through the mixed programming of the C support host computer and MATLAB, the fuzzy reasoning fusion theory is applied to simulate the condition assessment and early warning of the underground diaphragm wall bridge. At the same time, the host computer realizes the functions of dynamic curve drawing and MySQL database storage, etc.

2. Related Work

Compared with the traditional wired test system in the detection of small and medium-sized underground diaphragm wall bridges, the underground diaphragm wall bridge monitoring system based on wireless sensor network has many advantages such as low cost, low power consumption, low maintenance and update costs, high reliability, and convenient installation. However, a major factor restricting the development of wireless sensor networks is the problem of energy supply [9–11]. Sensor nodes can actively obtain energy from the actual working environment and convert it into available energy for node work [12]. The energy in the environment is often a source of energy. Continuously, the working life of sensor nodes can be greatly extended, so this paper has important research value and significance for the design and research of wireless rechargeable sensor network nodes applied in the structural health monitoring of underground diaphragm wall bridges [13].

Liu et al. [14] proposed a wireless module monitoring system. They designed and built the wireless sensors that make up the system, and at the same time they incorporated intelligent processing. To demonstrate the computational power of the sensor, Blanks et al. [10] added a signal processing algorithm to the hardware acquisition device. Through a lot of laboratory researches, they installed a node

of wireless sensors on a bridge in the Alamosa Canyon and also deployed a wired monitoring system. At the same time, Scuro et al. [15] verified the function of the wireless sensor module and compared wired monitoring with wireless monitoring. Lin et al. [16] introduced the intelligent gateway system composed of hardware, software, and communication protocols in detail and conducted a field test on a farm. The experimental results proved that the gateway operates in the sensor network test of local and remote locations. It is normal, and it has achieved its function well. This paper draws inspiration from it and provides some ideas for the future design of the gateway.

The researchers introduced a wireless temperature monitoring system based on ZigBee technology, with multiple wireless sensors colocated in a common channel, and carried out practical tests on the whole system and proved the feasibility of the system through a large number of experimental data [17]. The use of CC2430 as the control unit is introduced, and the SimpliTI protocol is used to locate the wireless sensor network, and the experimental results prove that the system can locate the position coordinates within a certain error range [18]. Scholars introduced the application of Bluetooth technology in video transmission in detail, improved the error correction coding technology on the basis of the existing Bluetooth technology, and improved the video signal quality of Bluetooth technology in the wireless video communication system, so as to reduce the error in the transmission. Some experts put forward the use of GPS positioning technology combined with GSM (Global System for Mobile Communications)/GPRS (General Packet Radio Service) transmission technology in the design and implementation of the geographic display module in the intelligent line inspection system to design and implement specific location real-time management and monitoring functions [19–21]. However, based on the current wireless technology, the above transmission technologies have their own advantages, for the wireless network technology to be used in underground diaphragm wall bridges [22], but the above-mentioned wireless transmission methods are not enough to meet the application requirements.

3. Construction of a Model for the Influence of Slope Sliding on the Stability of an Underground Diaphragm Wall Bridge Foundation Based on a Wireless Sensor Network

3.1. Wireless Sensor Network Module. The wireless sensor network data acquisition equipment integrates sensors, signal processing units, power supplies, and wireless communication units and is responsible for collecting key information of underground diaphragm wall bridges, such as bridge deck vibration, stay or suspension cable vibration, and local structural strain, temperature and humidity changes, wind speed, and other signals. The monitoring center $G(t)$ controls the wireless data $g(d, t)$ acquisition equipment to perform data acquisition and wireless transmission through relevant command information $p(t)$ and completes data

storage $p(r)$, management, analysis and processing, and early warning.

$$G(t)G(d) = \begin{cases} \frac{1}{4tr!(t-r)!}, \\ \frac{p(t)-p(r)}{g(d,t)}, \end{cases} \quad (1)$$

$$\frac{\text{lamda}(d,t)}{4tr!(t-r)(t+r)!} p(t) \in p(r,t,d). \quad (2)$$

There are multiple wireless data acquisition $t-r$ devices in the monitoring system $p(d)$ of the bridge structure of the line underground diaphragm wall, each wireless data acquisition device is a wireless sensor node, and the embedded technology is the key to the development of the sensor node. A node is a hardware system built by sensors, micro-controllers, memory, wireless modules, power supplies, and other devices. Embedded software realizes the logic control $\text{sigma}(d,t)$ of microcontrollers on other devices in the hardware circuit $cu(t)$, so that sensor nodes can complete data collection, storage, processing, and transmission.

$$\text{Sigma}(d,t) = p(t,r) * \frac{cu(t)}{2t(t-r)!}, \quad (3)$$

$$p(t,d) = \begin{cases} \frac{1.99d-1.2t}{2t(t-0.42)!}, \\ 1 - \frac{1.2t}{2d}, \end{cases} \quad (4)$$

In the underground diaphragm wall bridge structure monitoring system $p(t,d)$, each node needs to transmit the data to other nodes while collecting data and finally send it to the root node. Therefore, all nodes can only ensure the smooth completion of this process if they form a network. When designing the networking mode of the node, it is necessary to study the basic topology structure $ra(x) - ra(y)$ and select the appropriate networking mode according to the actual application scenario of the system $ak(x)$ and the wireless transmission performance of the node.

$$2\pi \overline{ra(x) - ra(y) - ca(x) - ca(y)} < \max \{ra(x) - ra(y)\}, \quad (5)$$

$$U(x) = \begin{cases} \frac{1}{2} ak(x) - \frac{u(s)}{a(s)}, \\ ak(x) - \frac{e(x)}{k(x)}. \end{cases} \quad (6)$$

The principle of the mesh structure $u(s)/a(s)$ is that each node is interconnected in a wireless manner and each node $e(x)/k(x)$ is connected to at least two other nodes to form a subnetwork, and these subnetworks are combined with each other. There are various communication paths between nodes in the mesh structure. When a node fails,

other nodes connected to it can change the route without causing a large-scale network failure. Therefore, the system stability $mx(r)$ of the mesh structure is high, and it also has good flexibility $w(r) - e(r)$ in the networking process.

$$\frac{n-d}{n+d} - \frac{r-e}{r+e} \in \frac{mx(r)}{w(r)-e(r)}, \quad (7)$$

$$ra(x) - ra(y) > 1 > ca(x) - ca(y). \quad (8)$$

First, the root node broadcasts a message packet containing its own address information $ca(x) - ca(y)$ to the surroundings. After the child node receives the broadcast message packet, it announces itself as a child node of the root node: then, these child nodes broadcast a message containing their own node number and find them in turn. In this way, as long as the nodes are arranged reasonably, whether it is a node with good communication quality or a node with poor communication quality, it will find a parent node that suits itself, and can receive control commands from the nodes in Figure 1, so that the entire network can work normally.

The sensor adopts force-balanced electronic feedback and mechatronics design, which can measure low-frequency and ultra-low-frequency signals. JBA12 has the characteristics of high precision, high sensitivity, high dynamic range and low frequency starting from 0Hz, flat frequency response, etc., which can well meet the requirements of vibration monitoring of underground diaphragm wall bridge structures. Among them, the sensor module and AD (Analog Digital) conversion module are mainly responsible for information collection and data conversion in the monitoring area; the microprocessor module is mainly responsible for controlling the entire sensor node to store and store the data collected by itself and the data sent by other nodes; the wireless communication module is mainly responsible for wireless communication with other sensor nodes or aggregation nodes and completes the control information exchange and data transmission and reception work; the power supply module provides the sensor nodes with the power energy required for operation, generally using miniature batteries. If the domain satisfies sparsity or compressibility, then, a measurement matrix that is not related to the transformation basis can be used to linearly project the transformed high-dimensional signal onto a low-dimensional space and then solve the optimization problem according to the relevant optimization algorithm.

3.2. Slope Sliding Structure Monitoring. In the slope sliding structure, a single wireless sensor network node is powered by a lithium battery with a voltage of 3.7V and a capacity of 800mAh. The wireless sensor module has a built-in tri-axial MEMS (Microelectromechanical Systems) vibration acceleration sensor and its corresponding conditioning circuit. The sensor module and the wireless transceiver module are connected through a connecting line to form a complete wireless sensor network node. The base station integrates the LT6908A wireless transceiver chip and its

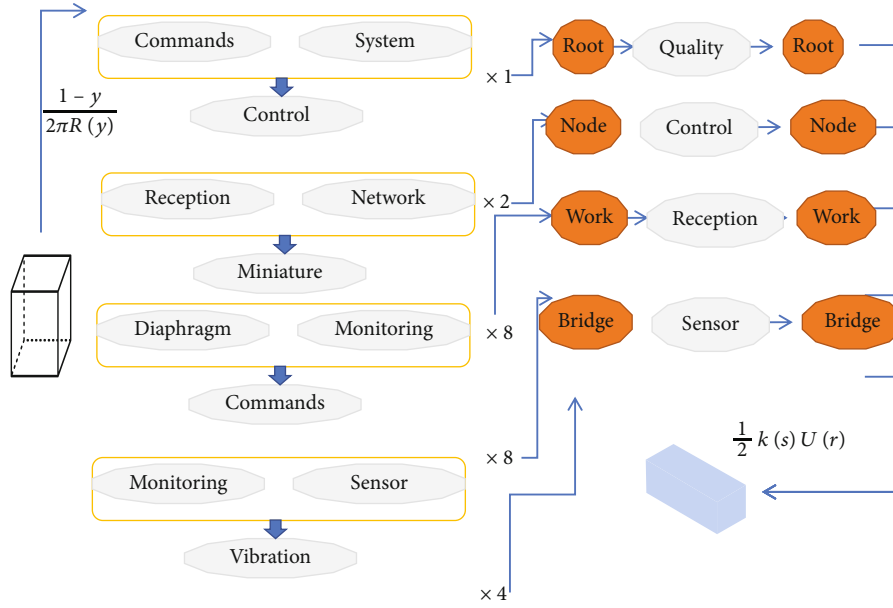


FIGURE 1: Wireless sensor network module design.

corresponding peripheral circuits, which are connected to the terminal PC using USB connection t2.

$$\frac{v(x)}{v(y)} = \frac{0.071x - 3.25}{0.031y + 1.35}, \quad (9)$$

$$W(x, t) = \frac{U(x)}{x} - \frac{I(x)}{x - t}. \quad (10)$$

This design uses the rail-to-rail operational amplifier TLC2254 to complete the function of low-pass filtering. It is powered by 3.3 V voltage and has 4 input and output channels. In addition, it has the advantages of low power consumption, low noise, and small size. Since the internal resistance of the output terminal of LIS344ALH is 110 K ohm, when the three-axis output signal is connected to the non-inverting input terminal of TLC2254, a capacitor can be connected in the middle. The formula for calculating the filter cutoff frequency of the output signal is as follows:

$$f(x, y, z) = \frac{1 - x}{2\pi RC(x, y, z)} - \frac{1 - y}{2\pi R(y)}, \quad (11)$$

$$\frac{52.2k\Omega}{4r!(1-r)(1+r)!} - 1 \in R(r). \quad (12)$$

In the actual measurement, the strain gauge needs to be pasted on the surface of the underground diaphragm wall bridge structure, when the measured structure produces strain. The strain gauge will also change accordingly, and eventually its resistance will increase or decrease. However, the resistance value cannot be measured directly. If the resistance is connected to the circuit, when the resistance value of the resistance increases or decreases, the voltage across its terminals will also increase or decrease accordingly. There-

fore, as long as the voltage is measured, the resistance change can be calculated.

$$\frac{\Delta r - 1}{4r!(1+r)!} - \frac{1 + \Delta r}{(1-r)!} \in U(r), \quad (13)$$

$$\begin{cases} \frac{u - 1}{4s!(1+s)!} - \frac{1 + u}{(1-s)!} = 1, \\ 1 - \frac{1}{2}k(s)U(r) = 0. \end{cases} \quad (14)$$

In addition, since the strain signal of the bridge structure of the underground diaphragm wall is a low-frequency signal and changes slowly, the amplified output voltage of the bridge needs to be filtered to filter out high-frequency signals and reduce signal interference. This design uses a high-speed, high-precision, rail-to-rail operational amplifier OPA350 to form a low-pass filter. The bridge output voltage signal is first amplified by AD620 and then filtered by a low-pass filter composed of OPA350. Finally, the filtered signal is connected to the analog sensor interface for AD conversion.

In order to improve the accuracy of the system in Table 1, the amplifier chooses a gain of 100. In addition, in order to avoid exceeding the range due to excessive structural strain, the system also needs to use a larger range. This design adopts two schemes of magnification 1000 times and 100 times. Therefore, according to the formula, the resistance value of the external connection resistance of AD620 can be calculated as 49.9Q and 499f2. The connection of the two resistances is switched by a double-pole single-throw switch, so that choose a different range. According to the formula, it can be calculated that the range of the strain gauge is divided into positive and negative 1000ue and positive and negative 10000ue, respectively. When the

TABLE 1: Slope sliding structure test.

Device name	Test voltage (mV)	Test current (mA)	Structure ratio
OPA350	28.65	16.47	0.43
OPA330	23.73	83.22	0.49
AD610	27.02	28.02	0.97
AD620	59.36	40.18	0.63
OPA360	79.52	86.30	0.66
AD630	46.04	59.34	0.03

strain value of the structure is small, the range of 1000ue is used.

3.3. Hardware Circuit Design. In the hardware design of the PCB (Printed circuit board) of the module, in addition to the factors such as reducing the size of the circuit board and making the wiring as simple as possible, it is also necessary to additionally consider the high-frequency line connected to the RF antenna. In order to ensure the normal operation of the module, the high-frequency line, power line, and ground line should be as thick as possible; especially for the VIN pin of the P2110B chip directly connected to the antenna, the wiring can be set to 50 ohms and as short as possible. The built system vibration signal acquisition and transmission reliability experimental platform is as shown, mainly including two functional areas of wireless transmitter and wireless receiver.

First, we set the standard sinusoidal signal parameters to be generated on the standard signal source and generate the standard sinusoidal signal, then open the wireless transceiver module, base station and human-computer interaction interface software, and issue work instructions. After each module is in working state, the input standard sinusoidal signal is sampled and transmitted wirelessly after buffering. The wireless receiving end receives the signal and uploads it to the PC through the buffering. The human-computer interface software on the PC ends the work after a period of work and is shown in Figure 2. After the experimental data is stored, the collected discrete data is analyzed in detail by the MATLAB computing software on the PC.

The purpose of power circuit design is to provide reliable working voltage for all working modules on wireless sensor network nodes. After analyzing the performance parameters of the above working modules, it is determined that the working voltage of the wireless sensor is 3.3 V, and it is powered by a 3.7 V lithium battery with a capacity of 800mAh, which can enable the wireless sensor network node to work continuously for more than 15 h, and the charging interface voltage is designed to be 5 V. The charging chip adopts TP4057 single-cell lithium battery charger chip. The chip adopts the battery positive and negative polarity reverse protection design. When working, it can use constant current/voltage linear control. It provides a status pin indicating the end of charging and an input voltage access status pin.

3.4. Stability Analysis of Underground Diaphragm Wall Bridges. Considering the design of the radio frequency cir-

cuit of the underground diaphragm wall bridge, the sensor node selects the relatively mature APC230 micropower wireless data transmission module as the wireless communication module. The APC230 module is a highly integrated half-duplex wireless data transmission module. The module itself is embedded with a high-speed microcontroller and a high-performance radio frequency chip ADF7020 and can set many channels. The step accuracy is 1 kHz, and the transmit power is as high as 100 mW. The APC230 module also innovatively adopts efficient cyclic interleaving error correction and detection coding, which can correct up to 24bits of continuous burst errors. The coding gain is as high as nearly 3 dBm, which is much higher than the general forward error correction coding, which greatly improves the anti-interference of the module. In addition, the module code also has reliable error detection ability, which can automatically filter out errors and false information and truly realize transparent connection.

From the packet loss rate in Figure 3, the order of delay from small to large is scheme 4, scheme 3, scheme 1, and scheme 2. The normalized network lifetimes are sorted in descending order of scheme 3, scheme 1, scheme 4, and scheme 2. Since the repeated coverage of the regular quadrilateral deployment is larger, it has higher reliability in theory; that is, the packet loss rate is smaller. The simulation results are consistent with the theory. Moreover, the IO port of the internal AD of the single-chip microcomputer has a low withstand voltage value. If the input voltage is too large, the IO port of the chip may be damaged, so the internal AD of the single-chip microcomputer cannot meet the requirements of this article. Therefore, this paper investigates an external AD conversion chip AD7606 to perform AD conversion of this node.

The packet loss rate and delay of scheme 3 and scheme 4 meet the usage requirements, and the difference is very small, and scheme 4 uses fewer nodes, so it is more cost-effective to deploy scheme 4. In the process of SPI (Serial Peripheral Interface) bus data transmission, if the size of the buffer register is eight bits, after 8 clock cycles, all data in the SPI buffer register on the microprocessor chip will be transferred to the SPI buffer register on the wireless transceiver chip. At the same time, the previous data in the SPI buffer register on the wireless transceiver chip is also transferred to the SPI buffer register on the microprocessor chip accordingly, which is like the SPI bus between the buffer register on the microprocessor chip and the wireless transceiver chip buffer register. A closed loop is formed, and the data in the buffer register is continuously cyclically shifted under the trigger of the clock cycle. An interrupt is generated when the number of shifts is equal to the number of bits in the buffer register.

4. Application and Analysis of the Influence Model of Slope Sliding on the Stability of Underground Diaphragm Wall Bridge Foundation Based on Wireless Sensor Network

4.1. WSN Data Extraction. The voltage data management unit is a part of the node hardware circuit. The input voltage

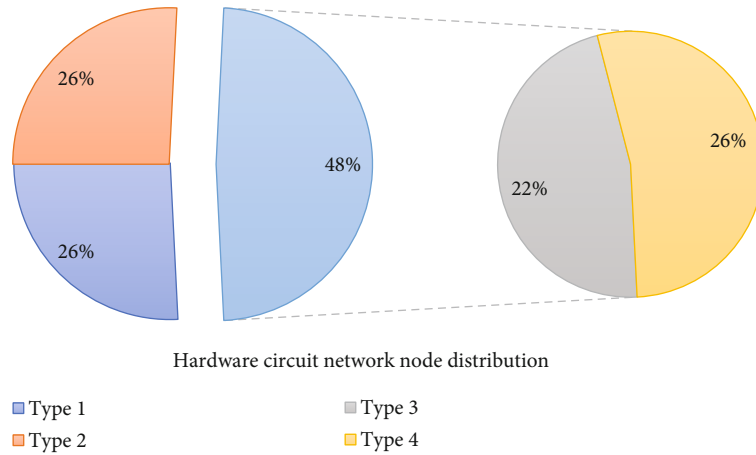


FIGURE 2: Distribution of hardware circuit network nodes.

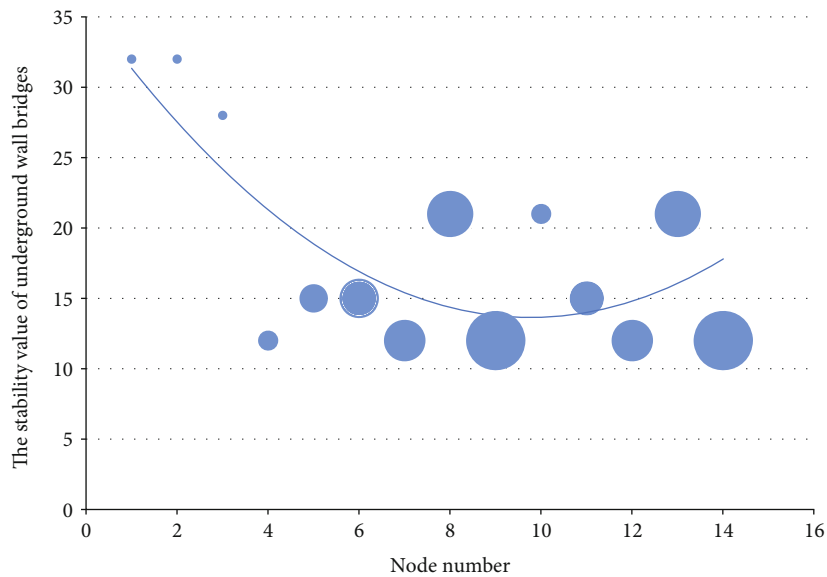


FIGURE 3: The stability of the underground diaphragm wall bridge.

of the node is divided into several voltages of different values by the power management unit to provide normal working voltage for each part of the node. According to statistics, the voltage values required by each part of the node are $\pm 12\text{ V}$, $\pm 5\text{ V}$, 3.3 V , and $\pm 2.5\text{ V}$. Since the input voltage provided by the battery is not regulated, it is in a dynamic range, and the voltage provided by the battery will continue to drop as the battery runs out of time, so it needs to be regulated first. The input voltage of the power module is designed to have a dynamic range of about 12 V . The voltage regulator module has high conversion efficiency, wide voltage input range, and good isolation and voltage regulation performance, which can well remove the noise of the input voltage at the node power supply end. HSD3-D12 converts the input voltage into $\pm 12\text{ V}$, and other voltages can directly convert the $\pm 12\text{ V}$ voltage into $\pm 5\text{ V}$, $\pm 2.5\text{ V}$ through the voltage regulator tube. In addition, HSD3-S3VS converts the input voltage to 3.3 V .

When deploying the nodes in Figure 4, due to the limitations of the on-site situation, it is often necessary to use some wired connections so that the wireless nodes can be deployed to a location that is more convenient for installation. The above solutions 1, 2, 3, and 4 are all solutions that do not apply to cables. In this paper, a system prototype is developed, including 1 gateway, 9 acquisition nodes, and 36 strain measurement points, and the wireless transmission range is more than 450 meters. In order to obtain the best deployment position of this prototype, in the case of using as few cables as possible (connecting the strain gauge measuring points with cables to both sides of the front of the underground diaphragm wall bridge is equivalent to increasing the sensing radius R), solution 5 was proposed. It adopts digital transmission technology and temperature and humidity sensing technology. The product has extremely high stability and reliability, and the product has fast response and anti-interference ability.

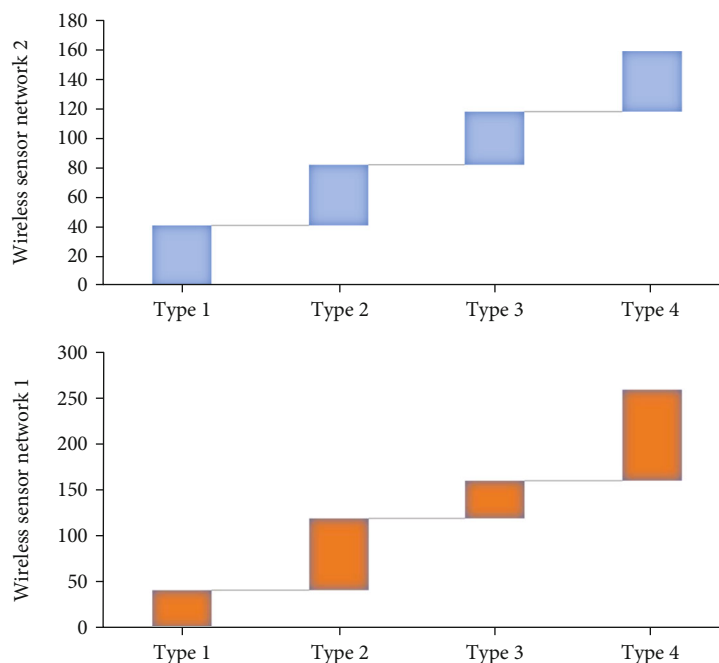


FIGURE 4: Data extraction from wireless sensor network.

The deployment scheme corresponding to the prototype of the research and development system in this paper is to measure 36 measuring points one at a time (it cannot cover the entire underground diaphragm wall bridge; the best scheme covering the entire bridge is scheme 4, which is only used as a reference for the deployment of the prototype). Taking a scheme similar to the above, the following approximate regular quadrilateral or regular hexagon scheme is obtained, and 9 nodes are deployed as evenly as possible at both ends of the bridge deck.

4.2. Wireless Sensor Communication Unit. The communication unit test cable, cable force adjustment device, and external environment excitation used in the test are the same as the communication unit wired sensor test, and the same set of data acquisition device is used for the cable force acquisition device. In the test, two node wireless sensors were used to test the vibration of the cable, which were placed at 2.50 m and 3.50 m, respectively. The arrangement of node on the cable is as shown. Since the battery plate at the bottom of node is curved and not completely horizontal, in order to better fix the wireless sensor on the test cable and avoid the relative sliding between the sensor and the cable, which will affect the authenticity of the collected acceleration data, the node is placed in the plexiglass mold, and then, the mold is firmly fixed on the cable.

In order to verify the complete wireless rechargeable sensor node signal acquisition and wireless charging work in the situation shown in Figure 5, this paper designs an experiment on a simulated bridge in the civil engineering laboratory and then conducts the actual work measurement of the overall wireless rechargeable sensor network node. In terms of signal acquisition, the data comparison analysis of wireless and wired methods is still used to verify, and the

wireless charging mainly analyzes and compares the charging effect by measuring the working power of the node and the charging power of the lithium battery.

The system consists of wireless sensor nodes installed on the bridge and remote data analysis, processing, and command terminals. The system realizes the communication management of bridge sensor nodes through 4G wireless mobile public communication network. A vibration experiment test was carried out; in terms of wireless charging, when the distance from the wireless rechargeable sensor node was 0.2 m, the radio frequency energy transmitter was used to charge and test the lithium battery powered by the node, and the voltage and current changes of the lithium battery were observed, and the measurement node was wireless. The working energy consumption of the communication phase and the nonwireless communication phase is used to evaluate the charging effect of Figure 6.

In order to simulate the increase of the vibration frequency of the diaphragm wall bridge when the internal structure of the diaphragm wall bridge is broken, the damping vibration of the elastic steel bar with a length of 29.4 cm is used to simulate the damping vibration of the diaphragm wall bridge under normal conditions.

The monitoring nodes are placed separately on the test platform to simulate the bridge deck, and the vibration excitation and stress-strain excitation are separately applied according to the test requirements. The relative error of the data packet loss rate and the cable force identification results under each working condition is analyzed, and the relative error of the identification results is not significantly different based on the acceleration data with and without data loss. The effect of the size on the accuracy of the recognition results is not obvious. This is consistent with the result obtained by using wired data to simulate the data loss

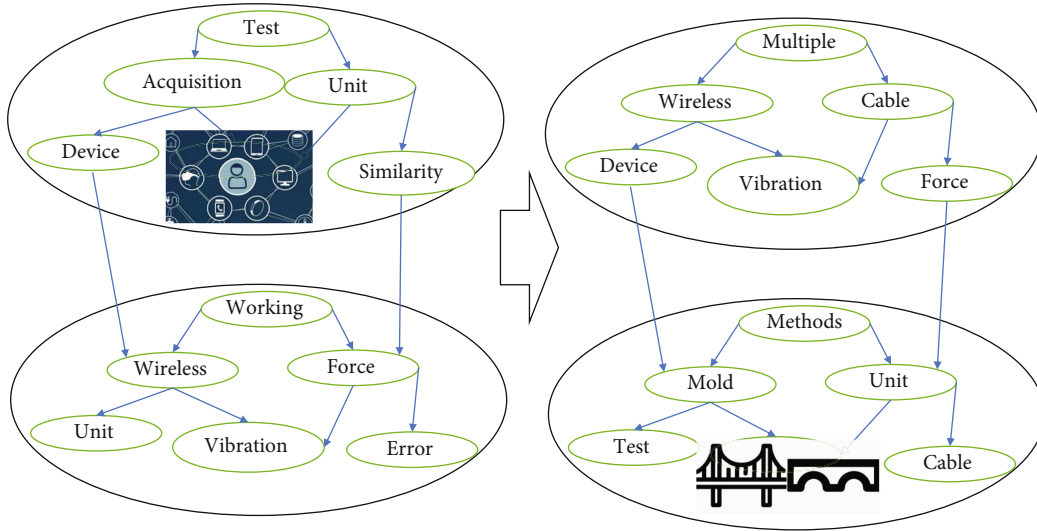


FIGURE 5: Wireless sensor communication topology.

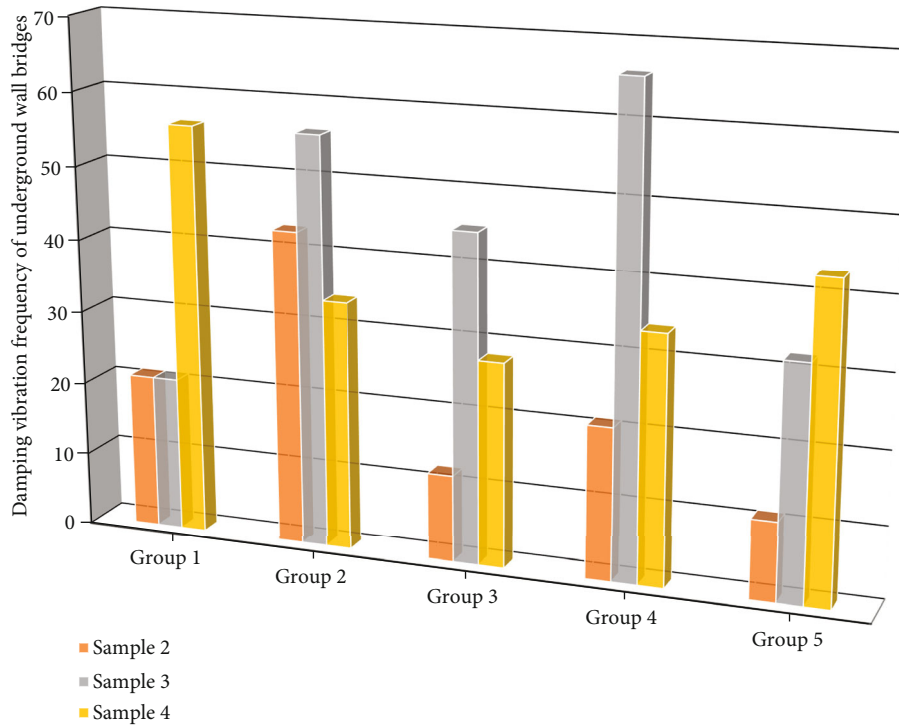


FIGURE 6: Damping vibration frequency of underground diaphragm wall bridge.

of wireless connection in the previous chapter, that is, when the data loss rate is within a certain range, the data loss has little effect on the accuracy of the final cable force identification result.

4.3. Simulation of Slope Sliding Structure. The underground diaphragm wall bridge monitoring system needs to work in a harsh environment. Here, the impact of the underground diaphragm wall bridge on-site environment on wireless communication is mainly considered. The main influencing factors of slope sliding are as follows: rainy weather, electro-

magnetic interference (from cars passing on the diaphragm wall bridge and their on-board electronic equipment, etc.), and obstacles (cars, pedestrians, and the structure of the diaphragm wall bridge, etc.). The simulation methods for these possible interference situations are as follows: change the parameters of the wireless propagation model in the simulation (shadow variance and path loss in the shadow model), disconnect the node for a certain period of time (some wireless electromagnetic interference can make the wireless node disconnection), and increase channel congestion (interference by same-frequency wireless technology).

The specific parameters are selected according to the empirical value recommendation of the NS2 simulation manual, the test results of relevant literature, and the actual test results of this study, as shown in Table 2.

Most of the monitoring environments of real underground diaphragm wall bridge structures are complex and interfere with each other, and the use of wireless connection is prone to data loss. By programming a new communication protocol in node and removing the antenna to test the transmission distance at the test site, the node produces data loss when monitoring the vibration of the cable.

The bridge model built in this paper is a T-shaped model of a simply supported beam with a length of 30 m at both ends and a width of 10 m. The three-dimensional finite element model of the built bridge is shown in the figure. The simply supported beam model consists of 127 nodes and 126 elements, and the bridge deck is composed of C30 concrete. The communication distance in the actual working environment may be very different from the theoretical communication distance in an open environment, and there will be subtle differences between different node individuals. Therefore, it is necessary to conduct field tests before using node to conduct experiments to find the optimal position of node arrangement and the optimal relative distance between the sensor and the base station, so as to ensure the smooth progress of the experiment and the collection of valid data. Due to the complex environment in the laboratory, in order to ensure a good communication environment, the sensor node and the base station are first connected to the external long antenna for testing.

4.4. Example Application and Analysis. It can be seen that the wireless sensor node mainly relies on two lithium batteries connected in series for charging, and the series voltage can reach about 7V, and then the boost and buck circuit designed in the power supply module of the node can meet the requirements of various types of chips on the node. By working voltage requirements, in order to study the effect of wireless charging on the energy supply of the entire node work, this paper mainly designs experiments to test the working power and energy consumption of the sensor nodes in Figure 7.

Among them, U is the power supply voltage of the circuit, and the voltage of two lithium batteries in series should be about 7.4V; I is the working current of the circuit. When performing different operations and each module is in a different state, the working current of the circuit is different. Since the power of the entire circuit board comes from the battery and we need to measure the working energy consumption of the entire board, the current I is selected to measure the total working current at both ends of the battery; t is the working time of the node. In the experimental operation, we use a set of multiple output DC power supply equipment to provide a stable 7.4V DC voltage for the wireless rechargeable sensor node and measure its working current in the non-wireless communication stage and the wireless communication stage, respectively.

Acceleration sensor technical indicators should meet the requirements. After investigation, the LIS344ALH accelera-

TABLE 2: Slope sliding architecture algorithm.

Slope sliding methods	Architecture algorithm codes
$I(x)/x$	Const double W = 0.4;
Data loss $f(x, y, z)$	Const double C1 = 2;
The underground diaphragm	Const double C2 = 2;
$4s!(1+s)!$	Const int ITER_NUM = 30;
Node disconnection $1-s$	Double calculatefitness (vector < double > x);
Wall bridge monitoring	Void freshvelocity(int i);
Work in a $1+u$	Void freshposition(int i);
Harsh environment	Population[i].m_x[j] = randrea
System needs to $2\pi R(y)$	Randreal(MIN_VELO[j], MAX_VELO[j]);
Wireless connection	Calculatefitness(population[i].m_x)
The use of $r+e$	Result = x[0] * x[0] + x [1] * x [1];
Is prone to $U(x)/x$	End

tion sensor chip of ST company is selected as the sensor chip of this article. The comparison of IS344ALH acceleration sensor chip technical indicators and specification requirements is shown. It can be seen that the acceleration sensor chip selected in this paper conforms to the technical specifications of bridge structure detection and meets the measurement requirements. The real-time frequency is 0.1 Hz, and the green stress-strain voltage curve is stable, and its value is about 1.4V. It can be seen that when the underground diaphragm wall bridge is static, the system only evaluates the state of the underground diaphragm wall bridge by the stress-strain data.

In the nonwireless communication stage and the wireless communication stage, the working power of the entire node is 890 mW and 1410 mW, respectively. From the experimental data in Figure 8, it can be seen that the charging power of the lithium battery is about 4.5 mW, which means that at the same time, the supply rate of power supply to nodes by wireless charging is 0.5% and 0.32%, respectively. From the data point of view, there are not many supplements for node power. This is also because wireless charging with electromagnetic radiation as the main method has certain energy dissipation in the transmission process, energy replacement, etc., but if it is used in some working power, a sensor network node with very low and simpler functional requirements will have a better charging effect. When the magnification is less than 1.58 times, that is, when the quality factor is lower than 0.707, the amplitude-frequency characteristics of the amplifier circuit are relatively stable, and there will be no jitter. Based on the results of the above experimental tests, the wireless rechargeable sensor network nodes cannot only achieve accurate acquisition of vibration acceleration signals of underground diaphragm wall bridges and wireless transmission and reception but also wireless charging using electromagnetic radiation, prolong the service life of the node, and supply the working energy of the node; especially for some wireless rechargeable sensor network

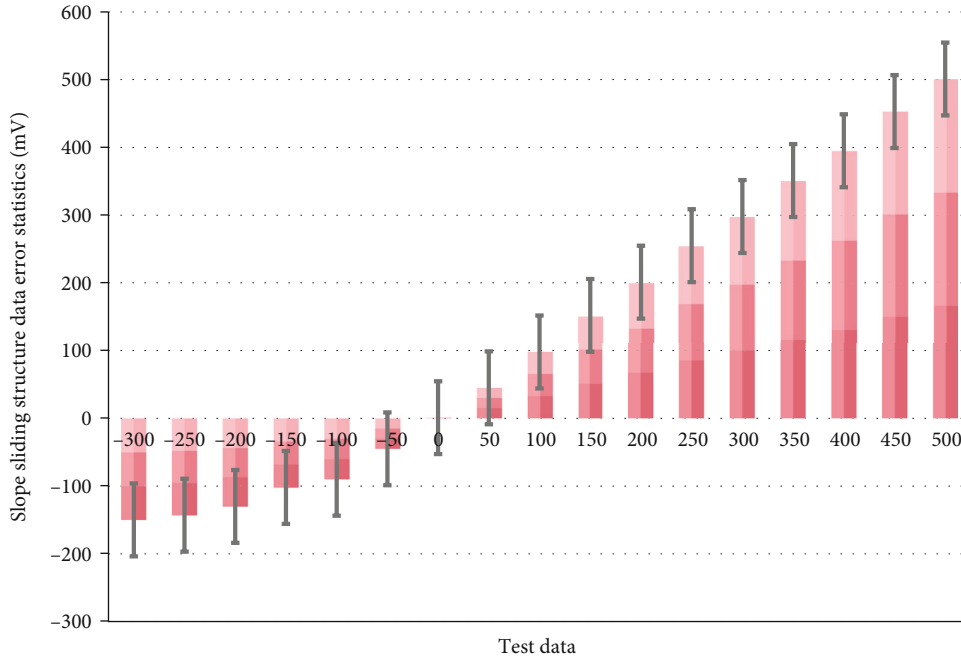


FIGURE 7: Data error statistics of slope sliding architecture.

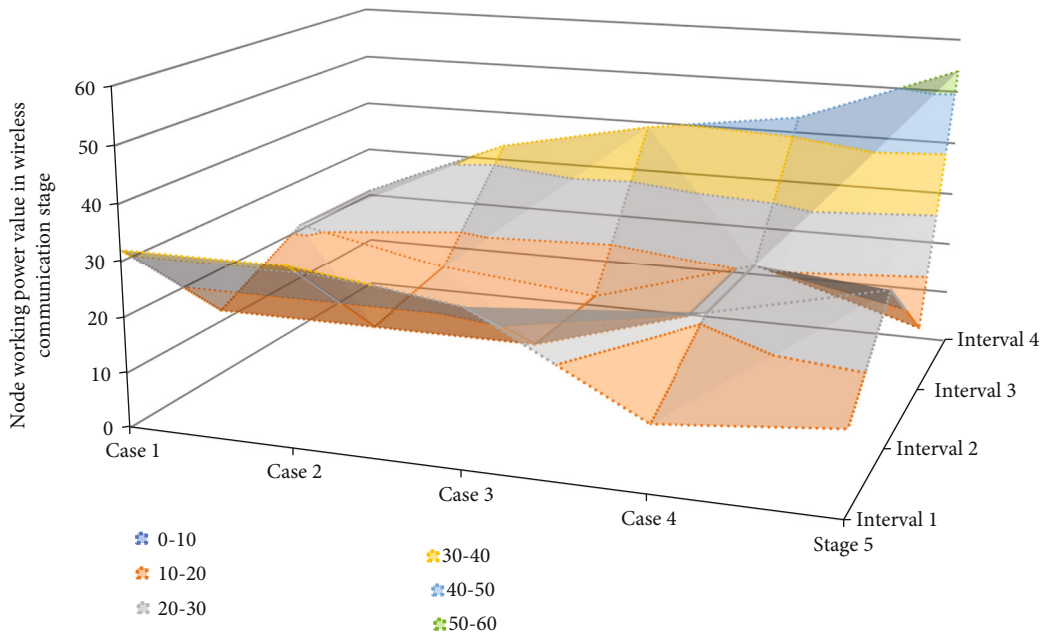


FIGURE 8: Node working power in wireless communication stage.

nodes with simpler functional structure and extremely low power consumption, the energy supply has greater energy supply.

5. Conclusion

Aiming at the singleness of information collected by wireless sensor nodes in the existing underground diaphragm wall bridge structure monitoring system, this paper develops a

full-featured wireless sensor system. The nodes integrate MEMS acceleration sensors and digital temperature and humidity sensors. The interface of the inclination sensor and the interface of the external acceleration sensor are designed, and the strain sensing unit is designed. The system can simultaneously collect the bridge deck vibration signal, local strain signal, inclination angle change signal, cable force signal of stay cable or suspension cable, and temperature and humidity change signal of underground diaphragm

wall bridges. The vibration monitoring node uses FPGA (Field Programmable Gate Array) to collect the frequency of the Pierce oscillation circuit where the PQCR-PSI structure is located and realizes functions such as temperature data collection, data processing, USB storage, and serial data transmission. Therefore, the monitoring system can comprehensively monitor the structure of underground diaphragm wall bridges and then comprehensively evaluate the safety status of underground diaphragm wall bridges, predict the structural damage of underground diaphragm wall bridges in advance, and reduce the occurrence of safety accidents of underground diaphragm wall bridges. This avoids the need to use multiple systems that can only monitor a single signal when comprehensively monitoring underground diaphragm wall bridges, thus greatly reducing the complexity of the entire monitoring project.

Data Availability

The data used to support the findings of this study are available from the corresponding author upon request.

Conflicts of Interest

The authors declare that they have no known competing financial interests or personal relationships that could have appeared to influence the work reported in this paper.

Acknowledgments

This work was supported by the National Nature Science Foundation of China (no. 41272333) and the National Program on Key Basic Research Project of China (Grant 2011CB013501).

References

- [1] H. Han, B. Shi, L. Zhang et al., "Deep displacement monitoring and foundation base boundary reconstruction analysis of diaphragm wall based on ultra-weak FBG," *Tunnelling and Underground Space Technology*, vol. 117, p. 104158, 2021.
- [2] J. Zhang, M. Li, L. Ke, and J. Yi, "Distributions of lateral earth pressure behind rock-socketed circular diaphragm walls considering radial deflection," *Computers and Geotechnics*, vol. 143, p. 104604, 2022.
- [3] F. Li, W. Qin, and H. Hu, "Experimental investigation monitoring the saturated line of slope based on distributed optical fiber temperature system," *Advances in Materials Science and Engineering*, vol. 2022, 13 pages, 2022.
- [4] J. Boštík, J. Štefaňák, and M. Závacký, "Transformation of the built environment for the rehabilitation of socially disadvantaged city districts," *Sustainable Rehabilitation and Risk Management of the Built Environment*, pp. 481–495, 2019, https://link.springer.com/chapter/10.1007/978-3-030-61118-7_39.
- [5] M. Grossi, "Energy harvesting strategies for wireless sensor networks and mobile devices: a review," *Electronics*, vol. 10, no. 6, p. 661, 2021.
- [6] K. Soga, A. Ewais, J. Fern, and J. Park, "Advances in geotechnical sensors and monitoring," *Geotechnical Fundamentals For Addressing New World Challenges*, pp. 29–65, 2019.
- [7] Z. Yang, S. Zhou, J. Zu, and D. Inman, "High-performance piezoelectric energy harvesters and their applications," *Joule*, vol. 2, no. 4, pp. 642–697, 2018.
- [8] B. Shi, D. Zhang, H. Zhu et al., "DFOS applications to geoenvironmental monitoring," *Photonic Sensors*, vol. 11, no. 2, pp. 158–186, 2021.
- [9] X. Zhu, Y. Zeng, W. Hu, X. Liu, and X. Zhou, "Experimental study on passive earth pressure against flexible retaining wall with drum deformation," *Engineering Letters*, vol. 29, no. 2, 2021.
- [10] M. Barzegar, S. Blanks, B. A. Sainsbury, and W. Timms, "MEMS technology and applications in geotechnical monitoring: a review," *Measurement Science and Technology*, vol. 33, no. 5, article 052001, 2022.
- [11] J. K. Sahota, N. Gupta, and D. Dhawan, "Fiber Bragg grating sensors for monitoring of physical parameters: a comprehensive review," *Optical Engineering*, vol. 59, no. 6, article 060901, 2020.
- [12] I. Vaníček, D. Jirásko, and M. Vaníček, "Interaction of transport infrastructure with natural hazards (landslides, rock falls, floods)," *Meas. Sci.*, vol. 2, no. 2–3, pp. 135–164, 2018.
- [13] E. Zlatanović, Z. Bonić, and N. Davidović, "Contemporary approaches to natural disaster risk management in geotechnics," in *Natural Risk Management and Engineering*, pp. 115–141, Springer, Cham, 2020.
- [14] L. Liu, X. Guo, and C. Lee, "Promoting smart cities into the 5G era with multi-field internet of things (IoT) applications powered with advanced mechanical energy harvesters," *Nano Energy*, vol. 88, p. 106304, 2021.
- [15] C. Scuro, F. Lamonaca, S. Porzio, G. Milani, and R. S. Olivito, "Internet of things (IoT) for masonry structural health monitoring (SHM): overview and examples of innovative systems," *Construction and Building Materials*, vol. 290, p. 123092, 2021.
- [16] W. Lin, M. Lin, X. Liu, H. Yin, and J. Gao, "Novelties in the islands and tunnel project of the Hong Kong–Zuhai–Macao Bridge," *Tunnelling and Underground Space Technology*, vol. 120, p. 104287, 2022.
- [17] Y. Liu, X. Li, H. Li, and X. Fan, "Global temperature sensing for an operating power transformer based on Raman scattering," *Sensors*, vol. 20, no. 17, p. 4903, 2020.
- [18] Z. Chen, W. Lu, P. Liu, Y. Yang, and L. Jiang, "Solid–liquid state transformable magnetorheological millirobot," *ACS Applied Materials & Interfaces*, vol. 14, no. 26, pp. 30007–30020, 2022.
- [19] D. Peduto, F. Elia, and R. Montuori, "Probabilistic analysis of settlement-induced damage to bridges in the city of Amsterdam (The Netherlands)," *Transportation Geotechnics*, vol. 14, pp. 169–182, 2018.
- [20] M. Li, X. Zhang, W. Kuang, and Z. Zhou, "Grouting reinforcement of shallow and small clearance tunnel," *Polish Journal of Environmental Studies*, vol. 30, no. 3, pp. 2609–2620, 2021.
- [21] S. S. Lin, N. Zhang, A. Zhou, and S. L. Shen, "Risk evaluation of excavation based on fuzzy decision-making model," *Automation in Construction*, vol. 136, p. 104143, 2022.
- [22] H. Yu, S. Li, and X. Wang, "The recent progress China has made in the backfill mining method, part I: the theory and equipment of backfill pipeline transportation," *Minerals*, vol. 11, no. 11, p. 1274, 2021.